

where  $F_0$  is given by eq 9 of the text and

$$\mathbf{F}_j = (F_{jA}, F_{jB}, F_{jC}) \quad j = 1, 2, \dots \quad (\text{A13})$$

with components  $F_{jA}$ ,  $F_{jB}$ , and  $F_{jC}$  as defined in eq 10. More explicitly, eq A12 reads

$$G(\theta) = (1 - \alpha_a + \alpha_b G_{1,B} + \alpha_c G_{1,C}) \times \\ (1 - \alpha_b + \alpha_b G_{1,A})(1 - \alpha_c + \alpha_c G_{1,A}) \quad (\text{A14})$$

$$G_{j,A} = (1 - \alpha_b + \alpha_b G_{j+1,A})(1 - \alpha_c + \alpha_c G_{j+1,A})$$

$$G_{j,B} = (1 - \alpha_a + \alpha_b G_{j+1,B} + \alpha_c G_{j+1,C}) \times \\ (1 - \alpha_c + \alpha_c G_{j+1,A}) \quad (\text{A15})$$

$$G_{j,C} = (1 - \alpha_a + \alpha_b G_{j+1,B} + \alpha_c G_{j+1,C}) \times \\ (1 - \alpha_b + \alpha_b G_{j+1,A}) \quad (\text{A15})$$

(for  $j < n - 1$ )

$$G_{n-1,A} = (1 - \alpha_b + \alpha_b \theta)(1 - \alpha_c + \alpha_c \theta)$$

$$G_{n-1,B} = (1 - \alpha_a + [\alpha_b + \alpha_c]\theta)(1 - \alpha_c + \alpha_c \theta)$$

$$G_{n-1,C} = (1 - \alpha_a + [\alpha_b + \alpha_c]\theta)(1 - \alpha_b + \alpha_b \theta) \quad (\text{A16})$$

Again the average number of offspring is obtained by differentiation at  $\theta = 1$ . This yields

$$G'(1) = \alpha_b G_{1,B}' + \alpha_c G_{1,C}' + (\alpha_b + \alpha_c) G_{1,A}' \quad (\text{A17})$$

The value for  $G_{1A}'$  results immediately for the first lines of (A15) and (A16)

$$G_{1,A}' = (\alpha_b + \alpha_c)^{n-1} \quad (\text{A18})$$

The evaluation of  $G_{1B}'$  and  $G_{1C}'$  is more involved. After some rearrangements one obtains

$$\alpha_b G_{1,B}' + \alpha_c G_{1,C}' = (\alpha_b + \alpha_c)^n + \\ 2(n-1)\alpha_b\alpha_c(\alpha_b + \alpha_c)^{n-2} \quad (\text{A19})$$

Inserting (A18) and (A19) into (A17) one finds the average number of offspring in the  $n$ -th generation  $\langle N \rangle_n$

$$\langle N \rangle_n = 2(\alpha_b + \alpha_c)^n + 2(n-1)\alpha_b\alpha_c(\alpha_b + \alpha_c)^{n-2} \quad (\text{A20})$$

Since the number of nodes in the  $n$ -th generation equals the number of paths of length  $n$  from the zero-th generation, the normalized path-length distribution is

$$h(n) = \frac{(1 - \alpha_a)^2}{\alpha_a(1 - \alpha_a) + \alpha_b\alpha_c} \{ \alpha_a^n + \alpha_b\alpha_c\alpha_a^{n-2} \} \quad (\text{A21})$$

where

$$\alpha_a = \alpha_b + \alpha_c$$

## Small-Angle Light Scattering of Reconstituted Collagen<sup>1</sup>

James C. W. Chien\* and E. P. Chang

Department of Chemistry and the Polymer Research Institute of the

University of Massachusetts, Amherst, Massachusetts 01002. Received April 21, 1972

**ABSTRACT:** Small-angle light scattering of reconstituted collagen films was photographed with  $H_V$ ,  $V_V$ ,  $V_H$ ,  $H_H$ , and intermediate configurations, where H and V refer to the direction of electric vector of the analyzer and the subscript denotes the polarizer direction. The effects of temperature, swelling, and deformation in the superstructures can be followed by observing changes in SALS. A deformation mechanism is presented detailing the various stages of strain-induced orientation. Cross-linked collagen film appears to contain smaller size scattering elements, which are more susceptible to orientation by swelling and temperature changes than those films which have not been irradiated. Films of collagen-poly(vinyl alcohol) copolymer gave SALS patterns nearly the same as the collagen homopolymer films. The grafted poly(vinyl alcohol), however, does not form new superstructural units, and it tends to plasticize the collagen units. Under high strain the molecules in reconstituted collagen film rearrange to form incipient "native" fibrils; the copolymer samples do not do so. When the sample is highly oriented, the polarized laser beam passing through it becomes depolarized. Light and phase contrast microscopy were also used to verify some of the SALS conclusions.

It is generally accepted that the basic constituent of collagenous substance is the tropocollagen triple-helical molecule which is about 3000 Å in length and 15 Å in diameter.<sup>2</sup> They aggregate in a solid state forming quarter staggered, fibrous long-spacing,<sup>3a</sup> or segment long-spacing<sup>3b</sup> crystallites. These in turn are assembled into long parallel bundles of fibrils such as those in rattail tendon. They are laid down in mutually perpendicular layers in the cornea. Therefore, there are several levels of superstructures, all having dimensions comparable to the wavelength of light. They

should scatter light efficiently as anisotropic rods or disks. A theory for the angular dependence of light scattering by a random assembly of such entities in two dimensions has been formulated by Stein and Rhodes.<sup>4</sup> This theory has been widely used in the interpretation of small-angle light-scattering (SALS) patterns. Recently, Kawai, *et al.*,<sup>5</sup> reported some SALS patterns obtained with films of acid-soluble collagen and enzyme-solubilized collagen. The conventional  $H_V$  and  $V_V$  configurations were used (the subscript designates that the electric vector of the polarizer is vertical, the letters H and V indicate the directions of the electric vectors of the analyzer). The fourfold symmetrical  $H_V$  pattern was found to be the (+)

(1) Presented in part at the American Physical Society Meeting, March 29, 1972, Atlantic City, N. J.

(2) H. Boedtker and P. J. Doty, *J. Amer. Chem. Soc.*, **78**, 4267 (1956).

(3) (a) J. H. Highberger, J. Gross, and F. O. Schmitt, *ibid.*, **72**, 3321 (1950); *Proc. Nat. Acad. Sci. U. S.*, **37**, 286 (1951); (b) F. O. Schmitt, J. Gross, and J. H. Highberger, *J. Exptl. Cell. Res., Suppl.*, **3**, 326 (1955).

(4) R. S. Stein and M. B. Rhodes, *J. Appl. Phys.*, **31**, 1873 (1960).

(5) M. Moritani, N. Hayashi, A. Utsuo, and H. Kawai, *Polym. J.*, **2**, 74 (1971).

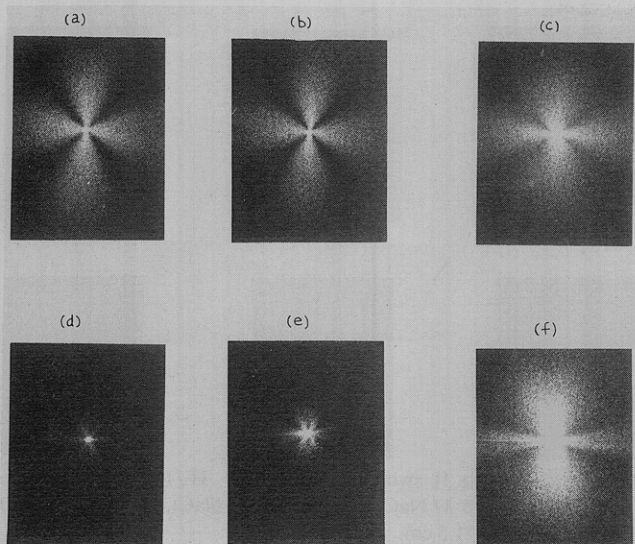


Figure 1.  $H_V$  pattern of sample II as a function of elongation: (a) 0%, (b) 8%, (c) 12%, (d) 24%, (e) 30%, (f) 40%.  $d = 23$  cm.

type—the intensity maxima are at 0 and  $90^\circ$  to the polarizer direction. The  $V_V$  pattern was circular in shape. Since  $H_V$  scattering originates predominantly from fluctuations in directional orientation of the optical axis, the observed patterns imply there is an angle of  $50$ – $70^\circ$  between the optical axis and the cylindrical axis of the rod. Both the above fluctuation and density fluctuation contribute to the  $V_V$  pattern. Since density fluctuation is azimuthal independent, the observed circular pattern implies that there is a dominant contribution by density fluctuation to  $V_V$  scattering. Swelling of the sample seemed to bring out some azimuthal-dependent  $V_V$  scattering, but the published patterns are of rather low quality. Deformation of the sample was not reported.<sup>5</sup>

Our work, the results of which are reported here, seeks to better define the superstructures of collagen, to observe the effects of stretching, heating, and swelling on this superstructure, and to understand the mechanism of deformation on a molecular level. An ancillary objective is to study how intermolecular cross-links and monomer grafting tend to modify the morphology of collagen.

### Experimental Section

Four synthetic materials, each derived from enzyme-solubilized collagen, were examined. They were films casted from the collagen (I), the same films with cross-links introduced by ultraviolet irradiation (II), and both unirradiated (III) and irradiated (IV) films prepared from collagens with poly(vinyl alcohol) graft. The samples were kindly provided by Dr. A. Rubin of the Cornell University Medical Center, New York, N. Y., and by Dr. T. Miyata of the Japan Leather Co. These same materials have been successfully employed by Dr. Rubin for implantation surgery.<sup>6</sup> The thickness of the film ranges from  $0.03$  to  $0.05$  mm. All the samples have low birefringence values<sup>7</sup> of about  $2 \times 10^{-4}$  in the relaxed state. In addition, measurements were made on native rattail tendon and on gelatin films (Knox brand).

Dry collagens films ( $\sim 5\%$  moisture) generally have  $10\%$  extensibility. It was found that by giving the sample blows of breath between successive stretching an ultimate elongation of as much as  $40\%$  can be achieved. About  $10$  min was allowed to elapse after the application of each additional extension prior to photographing the SALS pattern. This length of time is apparently sufficient for

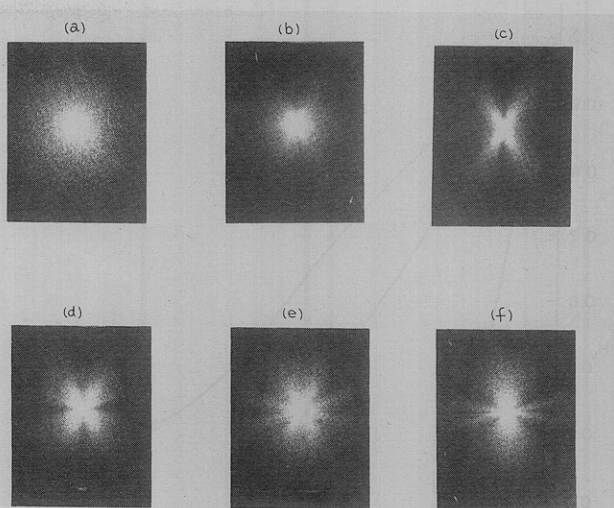


Figure 2.  $V_V$  pattern of sample II as a function of elongation: (a) 0%, (b) 8%, (c) 12%, (d) 24%, (e) 30%, (f) 40%.  $d = 23$  cm.

the sample to reach an equilibrium state, because no significant changes in SALS pattern were observed with longer time intervals.

The samples having dimensions of  $0.2 \times 2$  cm were stretched at a rate of about  $5\%/min$ . Measurements at subambient temperatures were made with the sample sandwiched between two copper blocks which were in turn enclosed in a rectangular glass container. Cold nitrogen gas served to lower the temperature, which was monitored by a thermocouple placed near the film. There was always frost accumulated on the windows of the glass container. That portion of the window in the path of the laser beam was defrosted by two preheated microscope cover glasses immediately before exposure. For elevated temperatures, a Mettler FP2 hot stage was used; temperature increment was set at  $0.2^\circ/min$ .

The SALS apparatus consisted of a SpectraPhysics continuous-wave He–Ne laser (Model 3000,  $\lambda$  6328 Å), a polarizer, and an analyzer. The scattering envelope was recorded on Polaroid film (Type 57) in a Polaroid cassette (Type 500). Most photographs were taken with  $H_V$  and  $V_V$  alignments, but  $H_H$ ,  $V_H$ , and other optical configurations were also occasionally used. The  $H_V$  scattering intensity was much weaker than the  $V_V$  intensity. Consequently,  $0.2$ -sec exposure time was used to record the  $H_V$  pattern as compared to only  $0.01$  sec for the corresponding  $V_V$  scattering.

Photographs were also taken with Polaroid negative films (Type 55), from which the relative scattering intensity was measured with a microdensitometer.

### Results

**Effect of Deformation of SALS.** The SALS patterns for sample II at various degrees of strain are given in Figures 1 and 2. The patterns for sample I closely resemble those for sample II. In the undeformed state, the  $H_V$  scattering is a (+)-type pattern designated as  $H_V$ -1 (Figure 1a). The maximum intensity is found along the direction of the transmitted ray, i.e., at zero scattering angle ( $\theta$ ). The intensity decreases monotonically with the increase of this angle (Figure 3). The variation is less steep for sample II than it is for sample I. The fourfold symmetry of the  $H_V$ -1 pattern is retained up to  $5\%$  elongation (Figure 1b); it is lost at  $12\%$  elongation (Figure 1c). The two lobes parallel to the stretching direction spread to include larger arcs of azimuthal angle  $\Omega$ , where  $\Omega$  corresponds to the angle in the  $yz$  plane measured from the  $y$  axis ( $z$  is the stretching direction). These lobes also are somewhat drawn in; the scattered intensity extends to smaller values of  $\theta$  than that of the horizontal pair. At  $25\%$  elongation (Figure 1d) the vertical lobes are clearly “split” into two pairs whose pattern is referred to as  $H_V$ -2. Additional strain causes further division of the horizontal lobes (Figure 1e).

(6) A. L. Rubin, R. R. Riggro, R. L. Nachman, G. H. Schwartz, T. Miyata, and K. H. Stenzil, *Trans. Amer. Soc. Artif. Int. Organs*, **14**, 168 (1968).

(7) J. C. W. Chien and E. P. Chang, *Biopolymers*, in press.



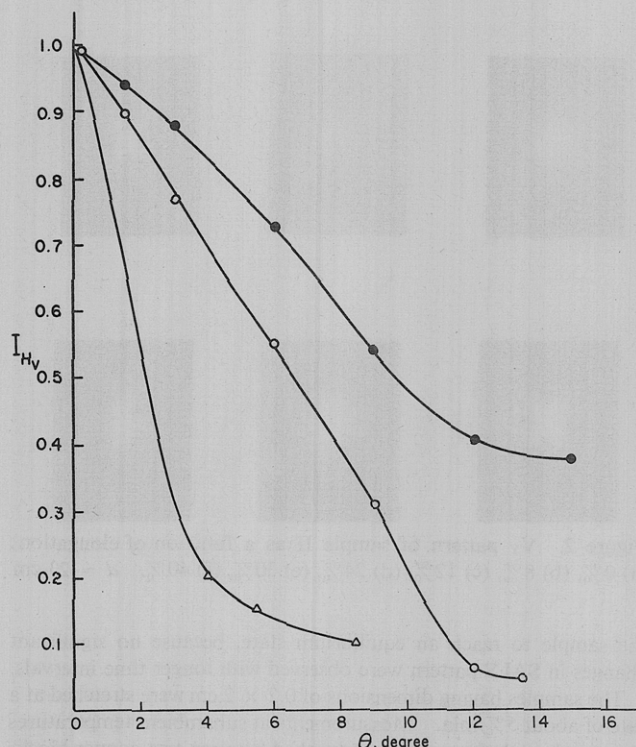


Figure 3. Variation of relative  $H_V$  scattering intensity with the scattering angle with the sample in the relaxed state: (○) sample I, (●) sample II, (△) calculated dependence<sup>5</sup> using the parameters  $L/\lambda = 40$ ,  $\omega_0 = 50$ , and  $R/L = 0$ , where  $L$  and  $R$  are the length and diameter of the asymmetric rod and  $\omega_0$  is the polarization angle.

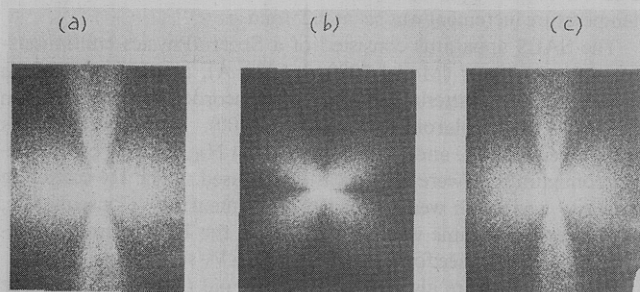


Figure 4. SALS patterns for collagen films at various per cent extension: sample II (a)  $V_H$ , 30%; (b)  $H_H$ , 12%; (c)  $H_H$ , 30%.

This pattern is called  $H_V$ -3. Finally, the two vertical pairs of lobes merged into one intense pair when the strain is 40% (Figure 1f). This pattern, which is referred to as  $H_V$ -4, is markedly more intense than the other  $H_V$  patterns. These data were obtained with the same exposure time and sample to film distance ( $d$ ).

In the unrelaxed state the  $V_V$  scattering is a circular  $V_V$ -1 pattern (Figure 2a). There is superimposed on it an extremely faint (X)-type pattern which has maximum intensity at  $45^\circ$  to the polarizer direction. The latter, designated as  $V_V$ -2, is clearly discernible for sample II at 8% strain (Figure 2b); it becomes evident only at 12% strain for sample I. At 12% elongation, the  $V_V$  pattern has its maximum intensity inclined about  $32^\circ$  from the polarizer direction, indicating some degree of perpendicular orientation. Additional strain causes the emergence of two new pairs of lobes along the horizontal direction (Figure 2e, strain about 25%). This eight-lobe pattern is referred to as  $V_V$ -3. At 40% elongation we obtain a  $V_V$ -4 pattern. It is very interesting that this  $V_V$  pattern bears

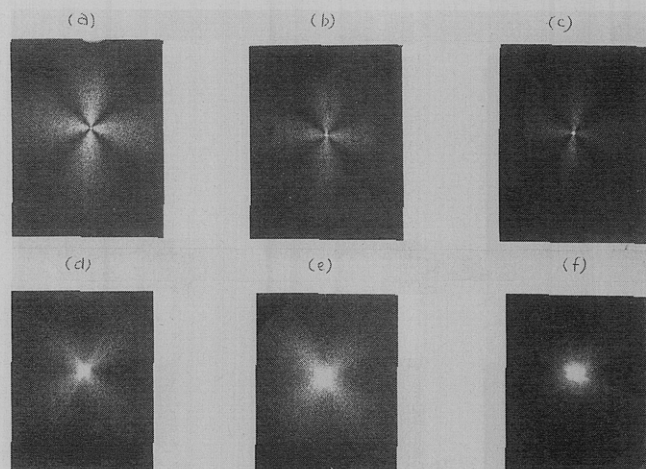
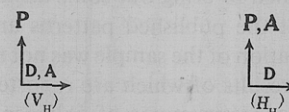


Figure 5. Sample II swollen with NaCl:  $H_V$  (a) 0.03 M NaCl, (b) 3 M NaCl, (c) 5 M NaCl;  $V_V$  (d) 0.03 M NaCl, (e) 3 M NaCl, (f) 5 M NaCl.  $d = 21.5$  cm.

striking resemblance to the corresponding  $H_V$ -4 pattern (compare Figure 1f with 2f).

A similar SALS strain dependence study was made on collagen-poly(vinyl alcohol) films (samples III and IV). In general, the trend in the change of scattering pattern is analogous to those described above for collagen samples I and II. There is, however, one principal difference—at 40% elongation the vertical lobes remain distinct for the copolymer samples, whereas they coalesce in the case of samples I and II.

In addition to the  $H_V$  and  $V_V$  scatterings,  $V_H$  and  $H_H$  measurements were also taken. The patterns for sample II are shown in Figure 4. The optical arrangements are



where  $D$  is the draw direction and  $P$  and  $A$  denote the electric vectors for the polarizer and the analyzer, respectively. Comparison of Figures 1, 2, and 4 establishes that the corresponding patterns of  $H_V$  vs.  $V_H$  and  $V_V$  vs.  $H_H$  at comparable deformation are the same aside from an expected  $90^\circ$  rotation.

**Effect of Salt Concentration on SALS.** Samples I and II were swollen in saline solutions for 24 hr. The NaCl concentration ranged from 0 to 5 M. The sample thicknesses for the two types of film were comparable at a given salt concentration, with the unirradiated samples (I) having a slightly higher degree of swelling. The SALS patterns were photographed under undeformed conditions, keeping the duration of swelling, exposure time, and  $d$  identical for each pair of samples (Figure 5).

The  $H_V$  scatterings are all of the  $H_V$ -1 type. At low salt concentrations, the scattering patterns are essentially the same as those of the dry samples (Figure 1a). The scattering intensities become increasingly weaker with the increase in NaCl concentration (Figures 5a–5c). Samples I and II respond similarly to swelling by saline solution of a given concentration.

All the  $V_V$  scatterings are superpositions of an intense  $V_V$ -1 pattern and a (X)-type  $V_V$ -2 pattern (Figures 5d–5f). For sample I, the  $V_V$ -2 pattern is already distinct after being swollen with  $H_2O$ ; it takes 24 hr of swelling with 0.1 M NaCl to reach the same stage for sample II. The pattern for sample I becomes increasingly diffuse with increasing concentrations of

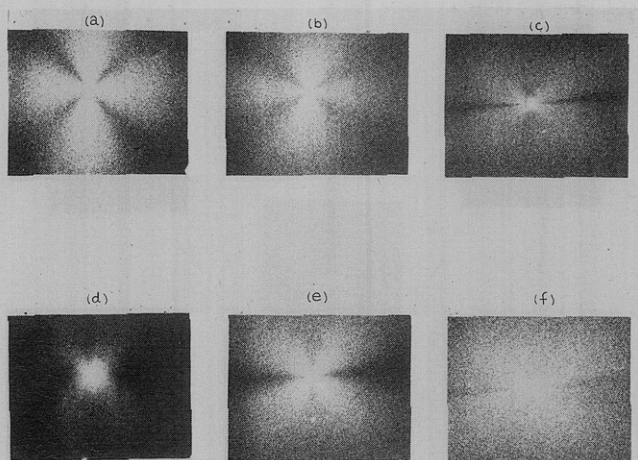


Figure 6. Saline solution (1 *M*) swollen collagen film II with various degrees of strain;  $d = 21.5$  cm:  $H_V$  (top) elongation (a) 0%, (b) 15%, (c) 30%;  $V_V$  (bottom) elongation (d) 0%, (e) 15%, (f) 30%.

NaCl; it becomes almost undiscernible at NaCl concentration of 3 *M* or higher. The corresponding pattern for sample II is best developed at 0.3 *M* NaCl; it is still visible at 5 *M* NaCl, though only barely.

In addition to swelling by saline solutions, the effect of glycerine was also investigated. The  $V_V$  pattern is almost circular; the  $H_V$ -1 scattering is quite weak.

**Strain Dependence of SALS in the Presence of Salt Solution.** Samples I and II were swollen in 1 *M* NaCl for about 48 hr. The SALS patterns for sample II photographed with various degrees of strain are shown in Figure 6. The responses to strain as reflected by SALS are very similar for the two types of films. However, the swollen sample of II is quite brittle and breaks beyond 30% extension.

The undeformed  $H_V$  patterns (Figure 4a) are basically similar for the swollen and the dry samples (Figure 1a), except that the former is much more diffuse (Figure 6a). However, the  $V_V$  scattering (Figure 7d) contains a distinct  $V_V$ -2 component. It is recalled (Figure 2a) that the corresponding  $V_V$  scattering for the dry samples gave only  $V_V$ -1 patterns.

Upon stretching, both the  $H_V$  and  $V_V$  patterns lose their fourfold symmetry. Deformation causes the lobes of the  $V_V$  pattern to move closer to the equator. The initial effect of strain on the  $H_V$  pattern is to increase the relative scattering intensity of the vertical lobes. At high strain, the  $H_V$  pattern closely resembles the  $V_V$  pattern (Figures 6c and 6f). The more complicated patterns observed with collagen films deformed in the dry state are conspicuously absent in this series of experiments.

The variation of  $H_V$  scattering intensity with the scattering angle was measured with a microdensitometer. By comparison, the scattering intensity falls off more rapidly with the scattering angle for the unirradiated sample (I) than for the irradiated sample (II). The scattering intensity of the  $V_V$  pattern was also measured in the direction perpendicular to the polarizer direction at a distance of 0.76 cm below the center of the incident beam. It is now sample II which shows the steeper decrease of scattering intensity with  $\theta$ .

An experiment was performed with collagen film stretched 30%, which gave the characteristic  $H_V$ -3 and  $V_V$ -3 patterns. The sample was then briefly soaked in saline solution while still under tension. The SALS photograph was taken again. In both instances, the scatterings returned to  $H_V$ -1 and  $V_V$ -2 patterns (Figures 7a,b,e,f). Parallel experiments were per-

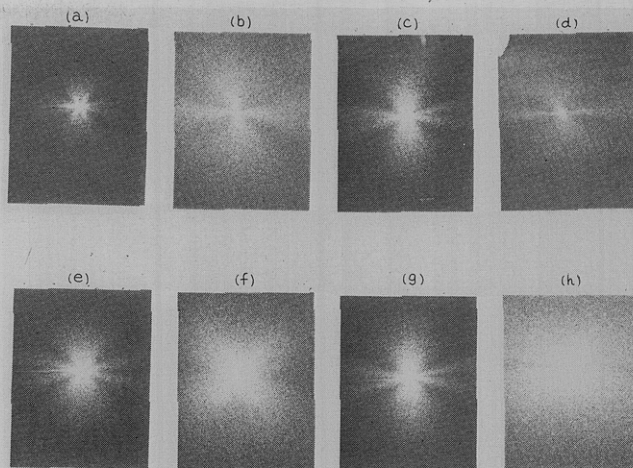


Figure 7. Effect of swelling with 1 *M* NaCl solution on prestretched collagen film:  $H_V$  30% extension (a) dry, (b) wet;  $H_V$  40% extension (c) dry, (d) wet;  $V_V$  30% extension (e) dry, (f) wet;  $V_V$  40% extension (g) dry, (h) wet.

formed for 40% stretched films (Figures 7c,d,g,h) with similar results.

**Effect of Temperature on SALS.** In our recent study<sup>7</sup> of the dynamic-mechanical dispersion of collagen films, it has been noted that the flow region occurs at about 220°. There was no distinct transition at about 145° corresponding to that extrapolated from dilatometric data by previous workers.<sup>8,9</sup> A major mechanical loss peak was however, seen at -80° for all collagen related samples. The effect of temperature was investigated to find whether similar structural alteration is manifested in SALS.

Because of experimental difficulties, measurement below -80° was not possible. The  $H_V$ -1 pattern diminishes in intensity with the lowering of temperature. This pattern disappeared almost completely for sample I at -80°. However, it was still very apparent for sample II at -67°, though with a significant reduction in intensity (Figure 8a). As the temperature is raised, the  $H_V$ -1 pattern becomes more prominent, further developed, and better resolved. It disappeared at 195° for sample I, but persisted to 216.5° for sample II (Figure 8h) until 217°, which is the flow temperature. It is interesting to note that the temperature at which  $H_V$  scattering of collagen-poly(vinyl alcohol) copolymer film vanishes is 210°.

The  $V_V$  scattering for sample I was not taken because of complications caused by density fluctuation. The corresponding scattering for sample II was collected, although the quality of the pattern was not too good. Nevertheless, it does show the development of a very weak  $V_V$ -2 pattern with heating, indicating that there is slight degree of thermally induced orientation which appears to reach a maximum between 100 and 120°. The scattering intensity diminishes with further heating. At the flow region, the  $V_V$  pattern becomes intense and circular.

**Strain-Dependent Birefringence of Collagen Films.** Birefringence of samples I and III was measured as a function of strain. The data are summarized in Figure 9. Both materials are characterized by three strain-optical regions: an initial region of large strain-optical coefficient at low elongation, followed by an intermediate region where the birefrin-

(8) P. J. Flory and R. R. Garrett, *J. Amer. Chem. Soc.*, **80**, 4836 (1958).

(9) L. P. Witnauer and J. G. Fee, *J. Polym. Sci.*, **26**, 141 (1957).



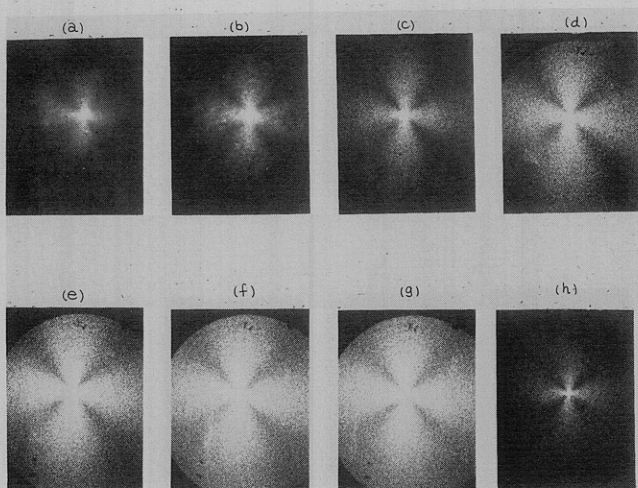


Figure 8. Effect of temperature on the  $H_V$  scattering of sample II,  $d = 23$  cm: (a)  $-67^\circ$ , (b)  $-37^\circ$ , (c)  $21^\circ$ , (d)  $70^\circ$ , (e)  $100^\circ$ , (f)  $150^\circ$ , (g)  $180^\circ$ , (h)  $216.5^\circ$ .

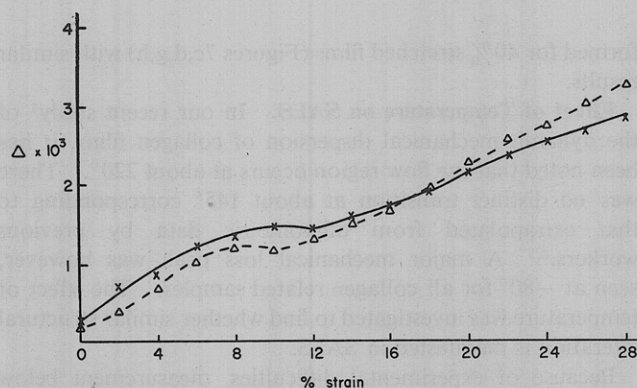


Figure 9. Variation of birefringence with strain for samples I (—) and III (---).

gence remains relatively constant, and a final region of rapid increase of birefringence with the increases of strain.

**SALS on Rattail Tendon and Gelatin.** In the undeformed state, collagen fibril of rattail tendon gives a random and stray  $V_V$  scattering, probably due to the uneven surface of the fiber which was not confined to a flat plane. Upon stretching, a horizontal periodic streak appeared which is the familiar fiber pattern. There are also a number of concentric rings due to diffraction caused by the pinhole. At fracture there is no distinct  $V_V$  scattering, but there is a weak  $H_V$  scattering where the lobes are inclined at  $55^\circ$  to the stretching directions.

**SALS at Large Film-Sample Distance.** SALS was measured at large film-sample distances with two objectives in mind. The fiber pattern reported for rattail tendon was obtained at  $d = 81$  cm; SALS of collagen film at comparable  $d$  could reveal fibrous structure not resolvable at small  $d$ . Furthermore, it would also be possible to detect small intensity differences between the individual lobes in a scattering pattern.

The results are given in Figures 10 and 11. At high elongation, the fiber pattern is clearly seen in all these photographs. Therefore, *highly stretched reconstituted collagen film and rattail tendon have very similar fiber structures.*

There are other significant observations. The SALS pattern is now clearly seen to be comprised of discrete spots, separated by distances much greater than the grain size of the photographic emulsion. They are different from the diffuse patterns normally observed with synthetic polymers.

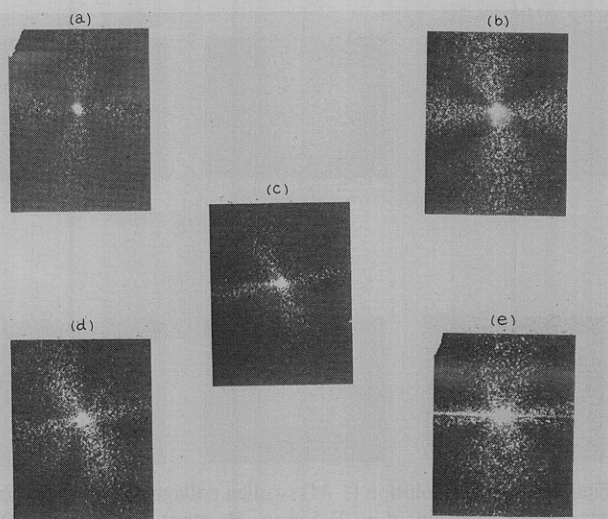


Figure 10. Variation of  $H_V$  patterns of sample I with strain at  $d = 101$  cm: (a) 0%, (b) 10%, (c) 20%, (d) 30%, (e) 40%.

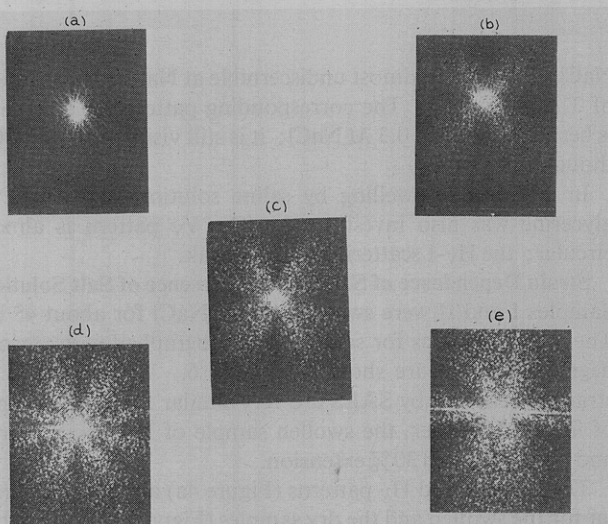
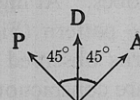


Figure 11. Variation of  $V_V$  patterns of sample I with strain at  $d = 101$  cm: (a) 0%, (b) 10%, (c) 20%, (d) 30%, (e) 40%.

The  $H_V$  and  $V_V$  patterns at 30 and 40% extension are nearly identical. The real significance of this observation became fully appreciated upon studying the patterns recorded with the following  $45^\circ$  optical configuration.



We shall first compare the  $45^\circ$  patterns in Figures 12a-d with the  $H_V$  patterns of Figures 1a,d,e,f, respectively, all photographed at  $d \sim 23$  cm. While the first two pairs are distinctly different, the second two pairs of photographs are virtually identical. When we compare the scattering patterns obtained at  $d = 101$  cm, we find that at low strain, the  $45^\circ$  patterns (Figures 12e,f) differ from the corresponding  $H_V$  patterns (Figures 10a,b) by a  $45^\circ$  rotation. On the other hand, the  $45^\circ$  patterns at high strain (Figures 12g,h) are obviously the same as the respective  $H_V$  patterns (Figures 10d,e). In fact, at 40% elongation, SALS patterns taken with any angle between P and A are identical. The similarity of SALS patterns for  $45^\circ$ ,  $H_V$ , and  $V_V$  arrangements implies that any effect due to birefringence will be small; the effect should be largest for  $45^\circ$  and smallest for  $H_V$  configuration.

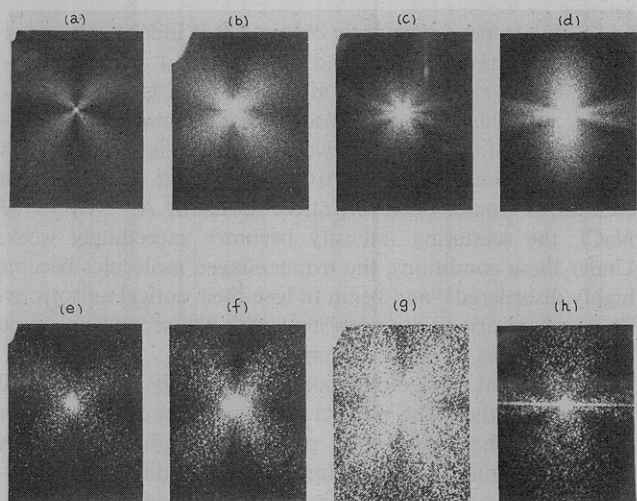


Figure 12. Variation of 45° patterns with strain for sample I:  $d = 22.5$  cm, (a) 0%, (b) 20%, (c) 30%, (d) 40%;  $d = 101$  cm, (e) 0%, (f) 20%, (g) 30%, (h) 40%.

The above observations may result either from depolarization or circular polarization of the light ray by the collagen film. To differentiate these, a mica quarter-wave plate was inserted between the sample and the analyzer both parallel and perpendicular to the stretching direction. No change in SALS was observed as the analyzer was rotated. In fact, the pattern is unaltered regardless of whether the quarter-wave plate is present or not. Therefore, the light ray has been depolarized by the collagen film.

The depolarization is, however, not total, as can be easily established by rotating the analyzer while observing SALS. Even though its azimuthal dependence remains unchanged, the absolute scattering intensity is sensitive to the orientation of the analyzer. There should be no intensity variations if the light is *completely* depolarized.

A further proof that SALS of highly orientated collagen film is independent of the analyzer is the fact that the same pattern is obtained with or without the analyzer. In these experiments, the photographic film records primarily the  $V_V$  scattering because of its greater relative intensity. Thus, in the absence of an analyzer and by rotating the polarizer, the SALS pattern is unchanged other than some slight variation in intensity.

When additional lobes appear in SALS as the result of deformation, a question may be asked whether this is the splitting of lobes in the undeformed pattern or whether a new pattern is emerging. The latter would be the case if one can observe changes in the undeformed pattern while the additional lobe is only beginning to emerge. We now return to inspect Figure 10, where frames b, c, and d clearly demonstrate this to be so. These  $H_V$  photographs establish without ambiguity that the  $H_V$ -1 pattern responds to deformation before the pattern becomes the  $H_V$ -2 type. Therefore,  $H_V$ -2,  $H_V$ -3, and  $V_V$ -3 are scatterings by two different entities. Furthermore, neither the stretching nor the transverse direction is a twofold symmetry axis (Figures 10b–d).

**Optical Microscopic Study of Collagen Films.** Observations described above indicate scattering entities which might be discernible by optical microscopy. A polarizing microscope was used to take a series of photographs of collagen films at various extensions with polarizer and analyzer perpendicular to each other. At 100× magnification, only fibrils can be resolved. The results show that they are highly oriented at 30 and 40% extension along the draw direction.

A phase contrast microscope was also used to study the orientation phenomenon. When the polarizer is parallel to the stretching direction, the refractive index fluctuation is quite random for the undeformed sample. At 10 and 20% elongation there are distinct orientation features which seem to indicate the preferred direction of orientation at some angle to the stretching direction. At 30 and 40% extension the refractive index variation is quite periodic parallel to the draw direction.

With the polarizer and stretching directions perpendicular to each other, the photographs tell the same story, except that the variation of refractive index between observed is along the transverse direction. At high elongation, there is closely spaced transverse order as expected.

### Discussion of Results

Stein and Rhodes<sup>4</sup> have formulated a theory for light scattering by a random assembly of anisotropic rods in two dimensions. This theory has been used to interpret the results obtained with polytetrafluoroethylene,<sup>4</sup> native cellulose,<sup>10</sup> collagen,<sup>5</sup> amylose,<sup>11</sup> hydroxypropylcellulose,<sup>12</sup> copolymers of chlorotrifluoroethylene and poly(vinylidene fluoride),<sup>13</sup> and block copolymers of styrene and ethylene oxide.<sup>14</sup> Recently, the theory has been extended to rods with finite thickness<sup>5</sup> and to three dimensions.<sup>15,16</sup> Our swelling studies<sup>7</sup> showed that collagen film has a planar orientation. Therefore, the two-dimensional theory<sup>4</sup> is valid and will be used as the basis to interpret our results.

The intensity of SALS for a random assembly of anisotropic rods, according to Stein and Rhodes,<sup>4</sup> should decrease monotonically with  $\theta$ . Its azimuthal dependence is determined by an angle  $\omega$  which is the direction of maximum polarizability for the rod as measured from the long axis of the rod. For  $\omega \approx 45^\circ$ , the  $H_V$  pattern should be of the (+) type with intensity maxima at 0, 90, 180, and 270° with respect to the polarizer direction. The  $V_V$  pattern, on the other hand, should be of the (X) type with intensity maxima at 45, 135, 225, and 315° with respect to the polarizer direction. The  $H_V$ -1 and  $V_V$ -2 patterns of collagen films display just such characteristics. Therefore, these materials are made of superstructures which scatter light as thin rods with 45° optical anisotropy.

SALS of the spherulite or anisotropic disk has its maximum at a certain scattering angle which is determined by the dimensions of the superstructure. It is relatively easy to calculate the radius from SALS data. Similar estimates for the anisotropic rod cannot be found readily. However, it is possible to use the length of the rod,  $L$ , as a parameter and find the best fit between the calculated and observed variation of scattering intensity with  $\theta$ . Use is made of the equations given by Stein and Rhodes<sup>4</sup> for the  $H_V$  and  $V_V$  scattering intensities.

$$I_{H_V} = p_0^2 L^2 \int_0^\pi N(\alpha) \delta^2 \sin^2 \alpha' \cos^2 \alpha' \frac{\sin(k\alpha L/2)}{(k\alpha L/2)} d\alpha \quad (1)$$

$$I_{V_V} = p_0^2 L^2 \int_0^\pi N(\alpha) (\delta \cos^2 \alpha' + b_v)^2 \frac{\sin(k\alpha L/2)}{(k\alpha L/2)} d\alpha \quad (2)$$

(10) J. Borch and R. H. Marchessault, *J. Polym. Sci., Part C*, No. 28, 153 (1969).

(11) J. Borch, A. Sarko, and R. H. Marchessault, *Bull. Amer. Phys. Soc.*, 16, 321 (1971).

(12) R. J. Samuels, *J. Polym. Sci., Part A-2*, 7, 1197 (1969).

(13) G. C. Adams and R. S. Stein, *ibid.*, 6, 31 (1968).

(14) J. J. O'Malley, Ph.D. Thesis, State University College of Forestry, Syracuse University, 1968.

(15) J. J. van Aartsen, *Eur. Polym. J.*, 6, 1095 (1970).

(16) N. Hayashi and H. Kawai, *Polym. J.*, 3, 140 (1972).



The definitions of all the parameters can be found in the reference<sup>4</sup> and will not be repeated here. The calculated results for  $L/\lambda = 40$  and a polarization angle of  $45^\circ$  are given in Figure 3. Comparison with microdensitometric readings gives an estimated rod length of  $5\text{--}6\ \mu$ .

The most interesting finding of this study is the change of SALS with deformation. At strain in excess of 10%, the overall SALS pattern is a superposition of two patterns. The possibility that this doubling effect is a manifestation of strain birefringence can be discounted. This kind of scattering should be the weakest in the  $H_V$  configuration and the most intense in the  $45^\circ$  configuration. This dependence is not observed experimentally.

Let us interpret the data by assuming that the sample consists of two kinds of scattering entities. One of these is almost certainly an assembly of tropocollagen molecules which will be referred to as type-A rods. SALS of these rods, randomly distributed, gives those patterns observed with the undeformed sample. Upon stretching, these rods become oriented along the direction of applied strain. If the new pattern which now emerges is attributed to scattering by type-B rods, according to the photographs they must be oriented in the perpendicular direction.

We have considered two possible origins for rod B. The first is that B and A are the same kind of superstructural entities differing only in their orientations. For some unknown reason deformation orients A rods along the stretching direction and B rods perpendicular to it.

A second possibility is that as more tropocollagen molecules are packed together with strain, there appears a transverse order which resembles thin anisotropic rods. There are reasons to favor this interpretation. The tropocollagen molecule is a dimorphic material consisting of alternating regions rich in polar and nonpolar residues, respectively. These segments are revealed in electron microphotographs<sup>17-19</sup> as "bands" which are receptive to staining agents, and "interbands" which are not. It is now commonly accepted that the bands correspond to the polar regions and interbands to the nonpolar regions. There are approximately 12 or 13 bands per 700-Å period in "native" collagen. Furthermore, the bands and interbands of the constituent tropocollagen molecules in native as well as SLS and FLS crystallites are in register. To a laser beam, these bands and interbands must appear to be anisotropic rods with diameters of about 20 and 40 Å, respectively. The actual dimensions, of course, vary with extension, particularly that of the polar region. The polar region is believed to be initially more disordered and, as a result, more deformable. It is plausible to identify B with these transverse rodlike superstructures. The axes of A and B rods should naturally be  $90^\circ$  when the bands and interbands are in register; the angle may be less than  $90^\circ$  if they are somewhat out of phase in a regular way.

The two possibilities can be differentiated experimentally. If the two anisotropic rods are the same, differing only in their orientations, then they should respond in a similar way to mild swelling treatment. In contradistinction, the transverse superstructures in the second case are held together by weak intermolecular forces. Consequently, scattering by B rods should be preferentially disrupted by swelling. The experimental results given in Figure 7 showed that the portion of

SALS due to perpendicularly oriented B is indeed eliminated by the swelling of prestretched sample with 1 M NaCl solution. However, the pattern attributed to A is largely unaffected. Similarly, Figure 6 showed that no new pattern is developed by deformation of a swollen film. It is clear that rods A and B respond differently to this treatment. More severe conditions would, however, affect SALS of A. With 5 M NaCl, the scattering intensity becomes exceedingly weak. Under these conditions, the tropocollagen molecules become highly disordered<sup>20</sup> and begin to lose their optical anisotropy. These observations are consistent with the second proposed superstructures for light scattering.

Beginning at 30% elongation and certainly at 40% in all experiments, the SALS pattern is independent of the analyzer direction. The light, after passing through these highly oriented samples, is depolarized. Because different components of the scattered light are mixed, and since the vertical component has the greatest intensity, a large increase in intensity would be expected for photographs taken with the  $H_V$  configuration. In other words, the  $H_V$  pattern in reality is a  $V_V$  pattern under these conditions.

Depolarization of the light by oriented collagen molecules is a direct consequence of the high optical rotatory property of collagen. The value of  $[\alpha]_{5890}$  is  $-360^\circ$ .<sup>21</sup> Light passing through the sample is rotated by an angle  $\rho$ , given by deVries<sup>22</sup>

$$\rho = \frac{\pi \Delta^2 P x}{4 \lambda^2}$$

where  $P$  is the distance for one helicoidal rotation of the optical axis,  $x$  is the distance traversed by light,  $\lambda$  is the wavelength, and  $\Delta$  is the birefringence of the region. The tropocollagen molecules in the sample are likely to be packed in different ways. They may be in register and parallel (SLS packing), in register but not necessarily parallel (FLS packing), or quarter staggered (native packing). Furthermore, these may differ in degree of overlap. Therefore, light traversing the sample should experience random rotations and counter-rotations and emerge depolarized.

The consequences of irradiation of collagen under a nitrogen atmosphere are decreases in optical rotation, some increase in average molecular length, and a significant increase in intrinsic viscosity. These changes were observed for the same enzyme-solubilized collagen with  $\gamma$  radiation.<sup>23</sup> Whereas the related experiments have not been performed with uv radiation, the nature of the molecular modification is probably similar. The SALS results on sample II appear to be consistent with materials containing intermolecular cross-links. For example, sample II seems to respond to smaller deformation than sample I. Cross-links should help to transmit forces exerted on the molecules.

The SALS patterns of collagen-poly(vinyl alcohol) copolymer are basically the same as the collagen homopolymer film, as is, also, their behavior under strain. There is no indication that the scattering elements in samples III and IV are not due solely to collagen. There are, however, two significant differences between the copolymer and homopolymer samples. At intermediate strain, the degree of orientation obtainable for the copolymer film is higher than for the homopolymer. Yet at high strain the SALS pattern was not transformed into one with intense perpendicular orientation

(17) F. O. Schmitt, C. E. Hall, and M. A. Jakus, *J. Cell. Comp. Physiol.*, **20**, 11 (1942); *J. Appl. Phys.*, **16**, 263 (1945).

(18) F. O. Schmitt and J. Gross, *J. Amer. Leather Chem. Ass.*, **43**, 658 (1948).

(19) A. J. Hodge in "Treatise on Collagen," Vol. 1, G. N. Ramachandran, Ed., Academic Press, New York, N. Y., 1967, Chapter 4.

(20) P. H. vonHippel and K.-Y. Wong, *Biochemistry*, **1**, 664 (1962).

(21) P. H. vonHippel and K.-Y. Wong, *ibid.*, **2**, 1399 (1963).

(22) H. deVries, *Acta Crystallogr.*, **4**, 219 (1951).

(23) K. Kohno, T. Nishihara, and E. Fukuda, *Jap. J. Appl. Phys.*, **9**, 1431 (1970).

(i.e., H<sub>V</sub>-4 and V<sub>V</sub>-4), nor was there a fiber component in the photograph. Apparently, the grafted PVA functions as a plasticizer which enables the collagen backbones to respond more readily to deformation and yet, at the same time, suppresses the packing of molecules into fibrils.

It was observed that swelling of relaxed collagen film with dilute saline solution brought out the V<sub>V</sub>-2 pattern even without stretching. This is in agreement with X-ray results. It is found<sup>24</sup> that the X-ray pattern (both low angle and high angle) shows disorientation when collagen fiber is dry and that the orientation improves markedly when the fiber is wetted. This has been interpreted to mean that there has been a stabilization of the helical structure. The polar kinks, which have slightly larger diameters than the nonpolar regions, are straightened out in the wet state. Our result indicates further that wetting also reduces density fluctuation, implying alignment of rods under strain-free condition.

There is a general trend of increasing scattering intensity with the increase of temperature. The thickening of sample

(24) M. A. Rongvie and R. S. Bear, *J. Amer. Leather Chem. Ass.*, **48**, 735 (1953).

may be responsible for this change. Heating also has a slight orientation effect, as evidenced by the appearance of a faint V<sub>V</sub>-2 pattern. As the sample was heated past 145°, there was no significant and sudden alteration of SALS pattern. Therefore, the crystalline melting point reported by some workers<sup>8,9</sup> for collagen–ethylene glycol must be a characteristic of that particular system. SALS disappears completely only when the actual flow temperature is reached.

In conclusion, this work has demonstrated that SALS is a powerful technique to study the morphology of collagen at both the protofibril and fibril levels and of their changes as induced by deformation, swelling, and heating. The results indicate that longitudinal as well as lateral alignment of collagen molecules can be revealed by the light-scattering patterns.

**Acknowledgment.** The authors are deeply appreciative to Professor R. S. Stein for his continuing interest in this work and for making the SALS apparatus available to us. This program is supported by the Public Health Service, National Institutes of Health Grant No. AM 14779.

## Stereospecific and Asymmetric Inclusion Polymerization. III. Polymerization of Substituted Butadienes Included in Racemic Perhydrotriphenylene<sup>1</sup>

Mario Farina,\* Guido Audisio, and Maria Teresa Gramegna

*Istituto di Chimica Industriale del Politecnico and  
Istituto di Chimica delle Macromolecole del Consiglio Nazionale delle Ricerche,  
Milan, Italy. Received May 10, 1972*

**ABSTRACT:** *trans*-2-Methyl-1,3-pentadiene, *trans*-3-methyl-1,3-pentadiene, 4-methyl-1,3-pentadiene, *cis,cis*- and *cis,trans*-2,4-hexadienes were polymerized by irradiation of their perhydrotriphenylene inclusion compounds. Polymers have head-to-tail *trans* 1,4 structures and in some cases show crystallinity and stereoregularity. *trans,trans*-2,4-Hexadiene and 2,5-dimethyl-2,4-hexadiene do not polymerize under the same conditions. By an analysis of the stoichiometry of the adducts, we attributed the behavior of said monomers to intermolecular steric factors, related to the different length of the included molecules and to the geometric constraints existing inside the channels. In the case of polymerizable monomers, the distance between unsaturated atoms of two successive molecules is shorter than 5.5 Å. This value represents the critical reaction distance for this type of polymerization and is considerably higher than that found in other cases.

The leading interest of our research presently concerns the inclusion polymerization of dienic monomers in the presence of the equatorial isomer of perhydrotriphenylene (PHTP) as host component. In the last years we published several papers on the synthesis<sup>2–6</sup> and the structural features<sup>7–9</sup> of perhydrotriphenylene and gave some preliminary informa-

tion on the radiation polymerization of several PHTP-included monomers.<sup>10–12</sup> In more recent papers, we described the stereospecific polymerization of *cis*- and *trans*-pentadiene<sup>13</sup> and studied the effect of both pressure and temperature on such polymerization.<sup>1</sup> In their turn, Allegra and Colombo, of this Institute, accomplished an X-ray analysis of the structure of a monocrystal of the PHTP–butadiene inclusion compound during polymerization.<sup>14</sup>

In this paper, we describe the results obtained using, as monomers, several substituted butadienes containing methyl groups in position 1, 2, 3, and/or 4. The aims of this research

\* To whom correspondence should be addressed at Istituto di Chimica Industriale dell'Università, 20133 Milano, Italy.

(1) M. Farina, G. Audisio, and M. T. Gramegna, *Macromolecules*, **4**, 265 (1971).

(2) M. Farina, *Tetrahedron Lett.*, 2097 (1963).

(3) M. Farina, G. Audisio, and P. B. Bianchi, *Chim. Ind. (Milan)*, **50**, 446 (1968).

(4) M. Farina and G. Audisio, *Tetrahedron Lett.*, 1285 (1967).

(5) M. Farina and G. Audisio, *Tetrahedron*, **26**, 1827 (1970).

(6) M. Farina and G. Audisio, *ibid.*, **26**, 1839 (1970).

(7) M. Farina, G. Allegra, and G. Natta, *J. Amer. Chem. Soc.*, **86**, 516 (1964).

(8) G. Allegra, M. Farina, A. Immirzi, A. Colombo, U. Rossi, R. Broggi, and G. Natta, *J. Chem. Soc. B*, 1020 (1967).

(9) G. Allegra, M. Farina, A. Colombo, G. Casagrande-Tettamanti, U. Rossi, and G. Natta, *ibid.*, 1028 (1967).

(10) M. Farina, G. Natta, G. Allegra, and M. Löffelholz, *J. Polym. Sci., Part C*, **No. 16**, 2517 (1967).

(11) M. Löffelholz, M. Farina, and U. Rossi, *Makromol. Chem.*, **113**, 230 (1968).

(12) M. Farina, G. Audisio, and G. Natta, *J. Amer. Chem. Soc.*, **89**, 5071 (1967).

(13) M. Farina, U. Pedretti, M. T. Gramegna, and G. Audisio, *Macromolecules*, **3**, 475 (1970).

(14) A. Colombo and G. Allegra, *ibid.*, **4**, 579 (1971).